Stability Enhancement of Grid-Connected Inverters Using Weighted Average Current Control Method

Akhavan, Ali; Vasquez, Juan C.; Guerrero, Josep M.

Published in:
IEEE Journal of Emerging and Selected Topics in Industrial Electronics

DOI (link to publication from Publisher):
10.1109/JESTIE.2021.3108511

Publication date:
2022

Document Version
Accepted author manuscript, peer reviewed version

This article has been accepted for publication in a future issue of this journal, but has not been fully edited. Content may change prior to final publication. Citation information: DOI 10.1109/JESTIE.2021.3108511, IEEE Journal of Emerging and Selected Topics in Industrial Electronics

Stability Enhancement of Grid-Connected Inverters Using Weighted Average Current Control Method

Ali Akhavan, *Member, IEEE*, Juan C. Vasquez, *Senior Member, IEEE*, and Josep M. Guerrero, *Fellow, IEEE*

***Abstract*- Among different factors that threaten the stability of *LCL*-filtered inverters in grid-tied mode, the variation of grid impedance and computational delay in digital systems are the most important ones. Often, a control system based on either the inverter- or grid-side current and a combination of impedance estimation and delay compensation methods are used to deal with these challenges. Such control systems are quite effective, however, they often involve a quite high implementation complexity. Especially, computational and PWM delay causes a critical frequency, which may deteriorate the stability conditions in grids with varying grid impedance. To deal with this challenge, a robust approach based on a weighted average current control method is proposed in this paper. The suggested control system employs the point of common coupling (PCC) voltage as a control variable, which increases the system stability in weak grids. Thus, the control system does not need any delay compensation or grid impedance estimation methods, which in turn, simplifies the control system. The effectiveness of the proposed method is examined using the experimental results in different case studies.**

***Index Terms*— Grid-connected inverters, *LCL* filter, stability, voltage feedforward, weighted average current control.**

I. Introduction

Grid-connected inverters have been extensively employed for injecting the power from renewable energy resources into the grid. Basically, using a filter at the output of the inverter is inevitable for smoothing the output current. Among various kinds of filters, the *LCL* filter is gained popularity for its better harmonic attenuation and lower cost and size [1]. However, it faces also resonance hazard and hence, demands a damping solution to make the system stable [2]. An important aspect in the control of grid-connected inverters with the *LCL* filter, which is often based on either inverter-or grid-side feedback current, is the resonance damping. In recent years, different resonance damping approaches have been suggested in the literature. Among these approaches, active ones have received more attention as passive methods may cause a considerable power loss [3]–[9].

Both inverter- and grid-side current have their own advantages to be used as an outer loop. By selecting the grid-side current as a control target, the injected power into the grid could be controlled, directly [10]. In contrast, the inverter-side current could be used for inverter overcurrent protection [11], [12]. Also, supposing $1.5T_s$ (T_s = sampling period) delay in digital control systems, it is proved that a grid-side current controlled inverter can work stably, without any damping mechanism when the resonance frequency falls higher than $f_s/6$, where f_s is the sampling frequency [13]. However, for the case of controlling the inverter-side current as a target control, the stability condition is the opposite [12]. The robustness of this method is very poor in weak grids since the resonance frequency changes because of grid impedance variations and consequently, the resonance frequency might move into an unstable region. Therefore, using damping methods seems necessary to increase the system robustness and reliability.

Despite the higher efficiency, conventional active damping-based control systems are prone to instability because of the effect of the computational and PWM delay in digital systems. In fact, the real part of virtual impedance that is introduced by the active damping loop becomes negative at frequencies higher than $f_s/6$, so-called critical frequency, which might make the system unstable [13]. Compensation of the delay's negative effect is discussed extensively in literature. An FIR filter, a modified notch filter, and a biquad filter are proposed in [5], [14] and [15], respectively, to push the critical frequency toward higher frequencies by injecting a positive phase to the control system. However, it might increase the high-frequency noises. In [16], sampling instant is shifted to amend the delay effect. A repetitive-based control system is proposed in [17] to cope with delay's negative effect, which expands the critical frequency to $f_s/4$. However, this method may amplify noises since it has an infinite gain at the Nyquist frequency. Also, this method loses its performance when the resonance frequency moves higher than $f_s/4$. An observer-based method is suggested in [18] for current prediction and in this way, compensates for the delay effect, which increases the sensitivity of the control system to parameter variations and uncertainties. Also, a method based on double-sampling approach is suggested in [19] to reduce the delay's negative effect. Nonlinear control methods such as model predictive control (MPC) [20], and sliding mode control (SMC) [21] are other approaches that have been gained more attention in recent years. Although effective, these methods need an accurate dynamic model and an optimization algorithm, which complicate the control system. Thus, a powerful computational unit is demanded, which in turn, increases the costs. Also, the performance of these methods could be affected by uncertainties.

The above-mentioned methods are effective, however, they mostly make the system more complicated. Therefore, a

This work was supported by the VILLUM FONDEN under the VILLUM Investigator Grant 25920, Center for Research on Microgrids (CROM).

The authors are with the AAU Energy, Aalborg University, 9220 Aalborg, Denmark (e-mail: alak@energy.aau.dk; juq@energy.aau.dk; joz@energy.aau.dk).

This article has been accepted for publication in a future issue of this journal, but has not been fully edited. Content may change prior to final publication. Citation information: DOI 10.1109/JESTIE.2021.3108511, IEEE Journal of Emerging and Selected Topics in Industrial Electronics

simple method with high robustness is demanded. To address this challenge, a weighted average current (WAC) control method has been suggested [22]–[25]. The WAC method arranges a pole-zero cancellation and removes the resonance. Therefore, the order of the control system is reduced, and the tuning procedure is simplified since the resonance does not exist anymore. On the other hand, the critical frequency does not affect the system stability. Therefore, the control system could be designed with a higher control bandwidth in comparison with a three-order system. However, the value of the grid impedance should be known in the WAC method, which in turn increases the sensitivity of this method to grid impedance variations [26]. In fact, to design the control system, the grid impedance should be estimated, which is not straightforward in a real application, such as weak grids where the grid impedance changes widely. To deal with this challenge, a grid impedance estimation method [27], [28], can be incorporated into the WAC method. It, however, may not be a good idea as the key feature of the WAC method is its implementation simplicity. Moreover, Pan *et al.* [29] proved that despite the stability of the weighted average current in this method, both the inverter- and grid-side currents are critically stable. Therefore, to make this method reasonable for real applications, it should be improved to increase its robustness against grid impedance variations.

A WAC control method combined with capacitor current-based active damping is used in [30] and [31]. However, the grid impedance variations, as well as the effect of critical frequency on the system stability, need to be addressed properly. In [32], an *LCCL* filter is used, and using a single-loop current control method, the current flowing between two capacitors is controlled. In fact, the *LCCL* filter is a physical implementation of the WAC control method. Although effective, it increases the cost and also, the desired split proportion of capacitors makes the implementation of the system a challenging task.

A robust and simple method is therefore demanded, which stabilizes the control system and copes with non-ideal conditions in real applications such as delay and grid impedance variations. To fill in this gap, a WAC-based control system is proposed, which employs the point of common coupling (PCC) voltage as a feedforward variable and inherits the conventional WAC control merits. The proposed approach has a simple structure and offers a high robustness to grid impedance variations. The control system does not need any delay compensation or grid impedance estimation method, which is its superiority in comparison with inverter- or grid-side current and conventional WAC control methods. In this way, the system keeps its stability even if the resonance frequency goes higher than the critical frequency. Since the PCC voltage is normally used for synchronization of the inverter and the grid, this method does not need any extra sensor in comparison with other conventional methods, which in turn, saves the costs.

The rest of this paper could be summarized in what follows. Section II presents a schematic of the system under study and conventional WAC control issues are introduced briefly to formulate the problem. In Section III, the proposed WAC control system based on PCC voltage feedforward is introduced. The effectiveness of the suggested technique is analyzed and its validity is verified using the experimental tests in Section IV. Finally, Section V, concludes the findings in this paper.

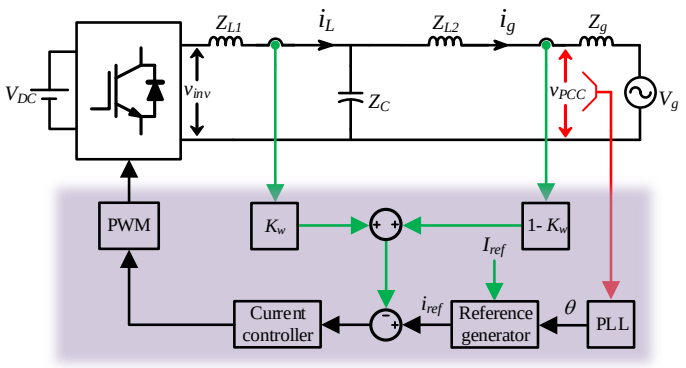

Fig. 1. Single-line schematic of a WAC-controlled inverter.

II. Schematic of the System

Fig.1 shows a single-line diagram of a WAC-controlled grid-connected inverter that is connected to the grid through a grid impedance Z_g. In this figure, Z_{L1} and Z_{L2}, are the impedance of the inverter- and grid-side inductors, respectively. Also, Z_C denotes the filter capacitor impedance. The grid impedance Z_g consists of inductance and resistance, however, since the resistive components offer passive resonance damping and make the system stable, they are neglected here to take into account the worst-case scenario. Equation (1) expresses these impedances in the Laplace domain.

$$Z_{L1} = L_1 s,\ Z_{L2} = L_2 s,\ Z_C = \frac{1}{Cs},\ Z_g = L_g s \tag{1}$$

As depicted in Fig. 1, both inverter-side and grid-side currents (i_L and i_g) are measured and weighted. Then, the made-up weighted average current could be used for control purposes.

Fig. 2 shows the per-phase control block diagram of the conventional WAC control method, where, the computation delay is modeled as z^{-1}. Also, the PWM delay that is caused by zero-order-hold (ZOH) effect can be formulated in the *s*-domain as follows [12].

$$G_{ZOH}(s) = \frac{1 - e^{sT_s}}{s} \tag{2}$$

Also, K_{PWM} models the inverter's transfer function and could be presented as

$$K_{PWM} = \frac{V_{DC}}{2V_{tri}} \tag{3}$$

where V_{DC} and V_{tri} are the amplitude of the DC-link voltage of the inverter and triangular carrier signal, respectively. $G_i(z)$ is the current controller. Also, K_w and 1-K_w are the weight factors for i_L and i_g, respectively.

This article has been accepted for publication in a future issue of this journal, but has not been fully edited. Content may change prior to final publication. Citation information: DOI 10.1109/JESTIE.2021.3108511, IEEE Journal of Emerging and Selected Topics in Industrial Electronics

$$T_w(z)=\frac{G_i(z)K_{PWM}}{\omega_r L_1(L_1+L_2+L_g)}\cdot\frac{\omega_r L_1 T_s(z^2-2z\cos(\omega_r T_s)+1)+(z-1)^2[K_w(L_1+L_2+L_g)-L_1]\sin(\omega_r T_s)}{z(z-1)(z^2-2z\cos(\omega_r T_s)+1)} \tag{4}$$

$$T_g(z)=\frac{G_i(z)K_{PWM}}{\omega_r(L_1+L_2+L_g)}\cdot\frac{\omega_r T_s(z^2-2z\cos(\omega_r T_s)+1)+(z-1)^2\sin(\omega_r T_s)}{z(z-1)(z^2-2z\cos(\omega_r T_s)+1)+K_w G_i(z)\dfrac{K_{PWM}\sin(\omega_r T_s)}{\omega_r L_1}(z-1)^2} \tag{7}$$

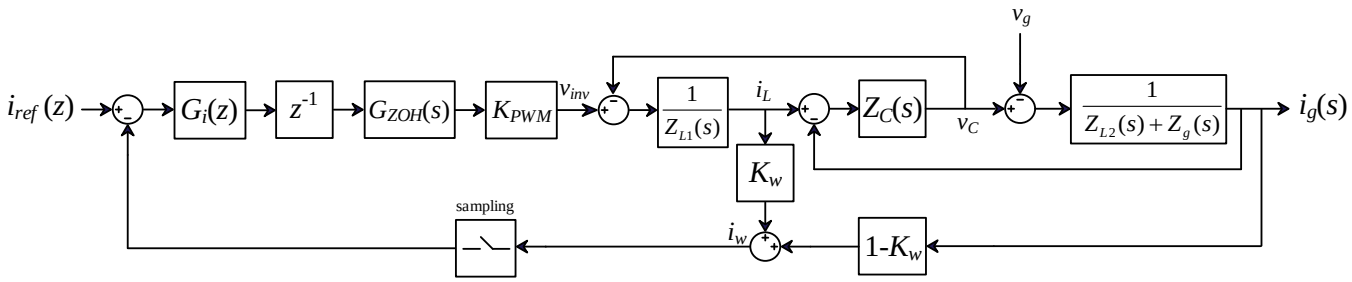

Fig. 2. The control system of the conventional WAC control method.

Regarding Fig. 2, the system loop gain where i_w (weighted average current) is the desired output, could be derived in z-domain as presented in (4) at the top of this page. According to (4), it could be concluded that if K_w tuned as

$$K_w=\frac{L_1}{L_1+L_2+L_g} \tag{5}$$

the system will have a pole-zero cancellation and thus, the loop gain could be simplified as

$$T_w(z)=\frac{K_{PWM}T_s G_i(z)}{z(z-1)(L_1+L_2+L_g)}. \tag{6}$$

From (6), it could be concluded that the system is not a three-order system anymore and it is degraded to a first-order system. In fact, it is similar to an L-filtered grid-connected inverter, in which the filter inductor value is $L = L_1 + L_2 + L_g$. In this way, i_w could be stabilized easily. This is the most important property of the WAC control method in comparison with inverter- or grid-side current control methods [22]–[24].

To use this merit, the grid inductance L_g should be known exactly. However, it may not be very straightforward in weak grid scenarios with varying grid impedance. Also, grid impedance estimation methods complicate the control system and they are not precise enough. Therefore, unknown and varying L_g causes that (5) fails and thus, the merit of the conventional WAC control method will be lost. However, even if the grid impedance is known exactly, the grid-side current i_g will be critically stable [29]. This problem is discussed in the following.

Regarding Fig. 2, the system loop gain where i_g (grid-side current) is the desired output, could be derived in z-domain as (7), as shown at the top of this page. It could be found that at the resonance frequency ω_r, where

$$\omega_r=\sqrt{\frac{L_1+L_2+L_g}{L_1(L_2+L_g)C}} \tag{8}$$

the loop gain could be simplified as

$$T_g(z=e^{\pm j\omega_r T_s})=-\frac{1}{K_w}\cdot\frac{L_1}{L_1+L_2+L_g}. \tag{9}$$

Supposing that L_g is known and $K_w = L_1 /(L_1 + L_2 + L_g)$, by substituting K_w in (9), $T_g(z=e^{\pm j\omega_r T_s})=-1$ achieves at the resonance frequency. It could be easily concluded that, although the weighted average current has been stabilized, the grid injected current is critically stable at the resonant frequency regardless of current controller gains and grid impedance value. It may cause a poor transient response and magnify the harmonic components around the resonance frequency. Therefore, the limitations of the conventional WAC control method could be summarized as: 1) the control system relies on the grid impedance and it should be known exactly and 2) the grid injected current is critically stable at the resonance frequency.

Fig. 3 depicts the closed-loop poles of the system when i_g is the target control, i.e., $T_g(z)/[1+ T_g(z)]$. In this analysis, L_g varies from 0 to 20 mH, and the parameters presented in Table I and Table II are used. It should be noted that in this figure, $K_w = L_1 /(L_1 + L_2)$ is considered and the poles introduced by the current controller are not shown since they do not affect the stability. As shown in Fig. 3, when $L_g = 0$, two resonant poles are exactly located at the border of the unit circle, which shows the critical stability. However, these poles go outside the unit circle for $L_g < 10$ mH and then return inside by further increasing of L_g. From these results, it can be concluded that the conventional WAC control method is not robust in weak grids, where the grid impedance varies widely.

Fig. 4 depicts the poles of the closed-loop transfer function of i_g, supposing that L_g is known and $K_w = L_1 /(L_1 + L_2 + L_g)$ is considered. As shown in this figure, the resonant poles go along with the unit circle border by increasing L_g, which implies that the grid injected current is critically stable in the conventional WAC control method, even if the grid impedance is known exactly.

This article has been accepted for publication in a future issue of this journal, but has not been fully edited. Content may change prior to final publication. Citation information: DOI 10.1109/JESTIE.2021.3108511, IEEE Journal of Emerging and Selected Topics in Industrial Electronics

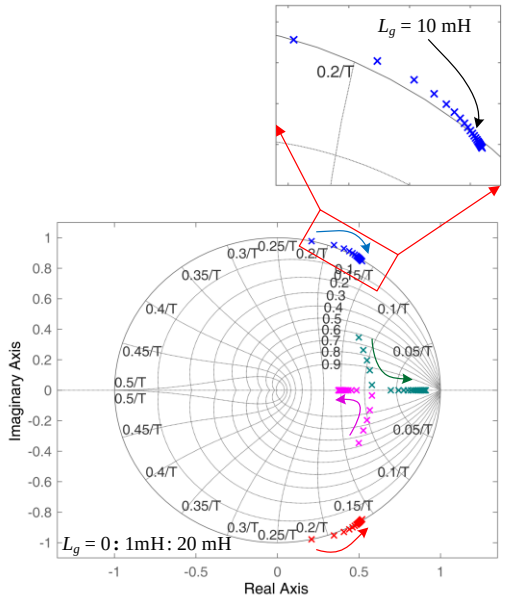

Fig. 3. Closed-loop poles map of i_g with the conventional WAC control method under the grid impedance variations and fixed K_w.

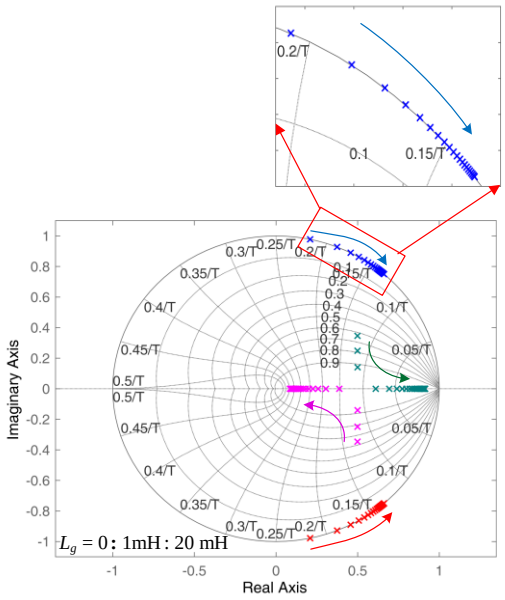

Fig. 4. Closed-loop poles map of i_g with the WAC control method under the grid impedance and known L_g.

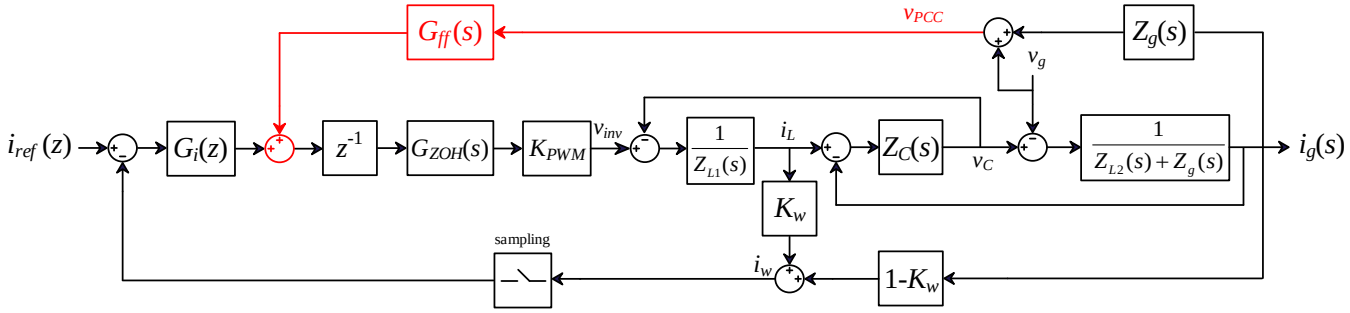

Fig. 5. The control system of the proposed WAC control method.

Figs. 3 and 4 verify the analysis presented in this section. Therefore, an improved WAC control method is demanded with high robustness, which does not depend on the knowledge of grid impedance.

III. Robustness Improvement of WAC Control Method

In this paper, a feedforward-based method using the PCC voltage is employed to enhance the robustness of the conventional WAC control method, while it does not need any knowledge about the grid impedance.

A. Proposed Control System

The block diagram of the proposed WAC control method is illustrated in Fig. 5, where v_{PCC} is the PCC voltage, and $G_{ff}(s)$ is the feedforward term for the PCC voltage loop. The loop gain of this control system, where i_w is the target control is obtained in the *s*-domain as shown in (10) to describe the proposed method easily.

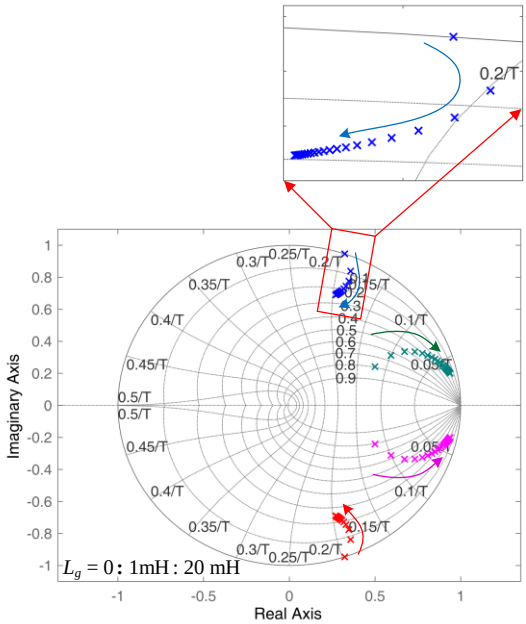

Fig. 6. Closed-loop poles of i_g with the proposed WAC control method under the grid impedance variations and fixed K_w.

This article has been accepted for publication in a future issue of this journal, but has not been fully edited. Content may change prior to final publication. Citation information: DOI 10.1109/JESTIE.2021.3108511, IEEE Journal of Emerging and Selected Topics in Industrial Electronics

$$T_{w\_ff}(s)=\frac{G_i(s)G_d(s)K_{PWM}}{Z_{L1}+Z_{L2}}\cdot\frac{Z_{L1}Z_{L2}+Z_{L1}Z_C+Z_{L2}Z_C+Z_{L1}Z_g}{Z_{L1}Z_{L2}+Z_{L1}Z_C+Z_{L2}Z_C+Z_{L1}Z_g+Z_CZ_g(1-G_d(s)G_{ff}(s)K_{PWM})} \tag{12}$$

$$T_{g\_ff}(z)=\frac{G_i(z)K_{PWM}}{\omega_r(L_1+L_2+L_g)}\cdot\frac{\omega_rT_s(z^2-2z\cos(\omega_rT_s)+1)+(z-1)^2\sin(\omega_rT_s)}{z(z-1)(z^2-2z\cos(\omega_rT_s)+1)+K_wG_i(z)\frac{K_{PWM}\sin(\omega_rT_s)}{\omega_rL_1}(z-1)^2-G_{ff}(s)\frac{L_gK_{PWM}}{L_1+L_2+L_g}(1-\cos(\omega_rT_s))(z^2-1)} \tag{14}$$

$$T_{w\_ff}(s)=\frac{G_i(s)G_d(s)K_{PWM}[Z_C(s)+K_w(Z_{L2}+Z_g)]}{Z_{L1}Z_{L2}+Z_{L1}Z_C+Z_{L2}Z_C+Z_{L1}Z_g+Z_CZ_g-G_d(s)G_{ff}(s)K_{PWM}Z_CZ_g} \tag{10}$$

where the delay is modeled with $G_d(s)$ as follows.

$$G_d(s)=e^{-1.5T_s s} \tag{11}$$

By considering $K_w = L_1/(L_1+L_2)$ or equivalently $K_w = Z_{L1}/(Z_{L1}+Z_{L2})$, $T_{w\_ff}(s)$ simplifies as (12), as shown at the top of this page. From (12), it could be found that if $G_{ff}(s) = 1/K_{PWM}$ is considered, the loop gain is almost free from the grid impedance and it could be approximated as

$$T_{w\_ff}(s)\approx\frac{G_i(s)G_d(s)K_{PWM}}{Z_{L1}+Z_{L2}}. \tag{13}$$

Therefore, using a PCC voltage feedforward method, the WAC control method improves so that K_w could be tuned without knowledge about grid impedance. It is worthy to note that since G_{ff} (or $1/K_{PWM}$) is just a function of the V_{DC} and V_{tri}, it is always fixed regardless of other control parameters.

The system loop gain is derived from Fig. 5, where i_g is the target control and it is presented in (14), as shown at the top of this page. For the control of the current in the outer loop, a proportional-resonant (PR) regulator is used as

$$G_i(s)=k_p+\frac{k_rs}{s^2+2\omega_is+\omega_o^2} \tag{15}$$

where $\omega_o = 2\pi f_o$ and f_o is the system nominal frequency and $\omega_i = \pi$ is selected as a cut off frequency.

The proportional gain k_p should be tuned to reach a desired crossover frequency f_c. The proportional gain could be designed according to [33]

$$k_p=\frac{2\pi f_c(L_1+L_2)}{K_{PWM}} \tag{16}$$

where, f_c is selected 0.05 f_s [34]. To reduce the impact of the resonant part at the crossover frequency, its corner frequency (i.e., $k_r/(2\pi k_p)$) is usually set as 0.1 f_c [35]. Hence, the resonant gain of the regulator can be designed as

$$k_r=\frac{2\pi f_c}{10}k_p \tag{17}$$

From (16), (17), and also, using system parameters in Table I, $k_p = 17$ and $k_r = 5000$ are yielded.

The PR regulator could be implemented using two integrators as explained in [36]. By discretizing the direct integrator by forward Euler and the feedback one, by backward Euler method, the PR could be obtained as (18) in the discrete form. Refer to [36] for more details about the discretization of the PR regulator.

TABLE I
Parameters of the inverter and grid

Parameters of inverter	
Input DC voltage, V_{dc}	650 V
Inverter-side inductor, L_1	3.6 mH
Filter capacitor, C	4.5 µF
Grid-side inductor, L_2	1.8 mH
Sampling and switching frequency	10 kHz
Rated power of inverter	2.2 kVA
Parameters of utility grid	
Grid Voltage, V_g (Phase-to-phase RMS Voltage)	400 V
Frequency	50 Hz
Grid inductance, L_g	$0 < L_g < 20$ mH

TABLE II
Control Parameters

Voltage controller	
k_p	17
k_r	5000
K_w	0.67
V_{tri}	$V_{DC}/2$
K_{PWM}	1

$$G_i(z)=k_p+k_r\frac{2T_s(z-1)\omega_i}{z^2+z(\omega_o^2T_s^2+2\omega_iT-2)-2\omega_iT_s+1} \tag{18}$$

B. Stability Investigation

The stability of the grid injected current is critical because it is the final output of the inverter. Therefore, it is examined with L_g varying up to 20 mH. The closed-loop poles of the system with i_g as the target control are illustrated in Fig. 6 [see the previous page]. As shown in this figure, the resonant poles are located at the unit circle only when $L_g = 0$, since in this situation, the loop gain of the conventional and proposed WAC control methods are exactly the same [see (7) and (14)]. However, these two critically stable poles move inside the unit circle by increasing L_g. Thus, the stability is guaranteed for all L_g except $L_g = 0$, which is critically stable. However, such a single point does not make a visible problem in practice because the parasitic resistances and skin effect offer some damping that thus, help the system to operate stably. On the other hand, the inverter rarely connects to a very stiff grid with zero grid impedance.

This article has been accepted for publication in a future issue of this journal, but has not been fully edited. Content may change prior to final publication. Citation information: DOI 10.1109/JESTIE.2021.3108511, IEEE Journal of Emerging and Selected Topics in Industrial Electronics

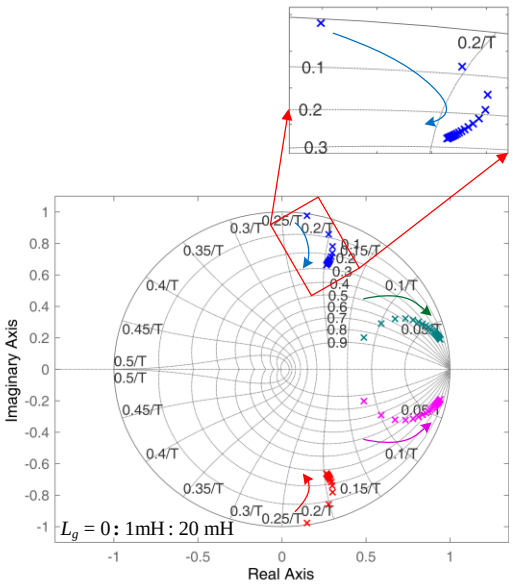

(a)

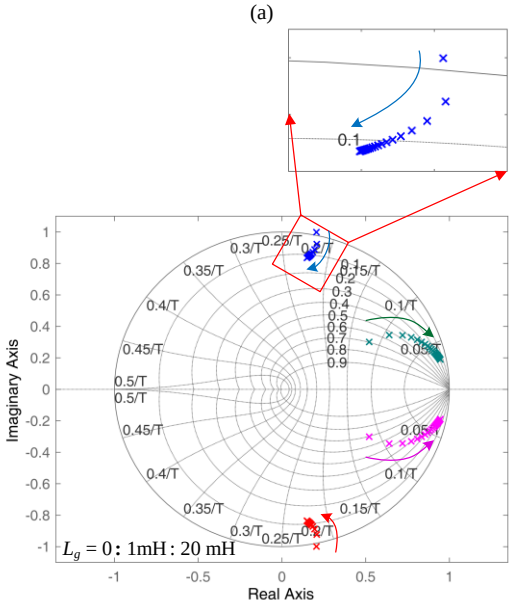

(b)

Fig. 7. Closed-loop poles of i_g considering ±20% tolerance of L_1 and L_2 with the proposed WAC control method under the grid impedance variations and fixed K_w. (a) Case A: L_1 = 1.2L_{1_nom}, L_2 = 0.8L_{2_nom}. (b) Case B: L_1 = 0.8L_{1_nom}, L_2 = 1.2L_{2_nom}.

C. Stability Investigation Considering Parameters Tolerances

As K_w = L_1/(L_1 + L_2) is a function of the L_1 and L_2, therefore, deviation of these parameters due to the tolerance or aging may affect K_w and in this way, it may affect the control system performance. In this part, the stability of grid-injected current is investigated considering the possible variations of L_1 and L_2. In practice, the variations of L_1 and L_2 are limited to ±20% [13]. Therefore, the closed-loop poles of (14) considering the variations of L_1 and L_2, with L_g varying up to 20 mH are examined. To this end, two worst-case scenarios are considered: Case A: L_1 = 1.2L_{1_nom}, L_2 = 0.8L_{2_nom}, and Case B: L_1 = 0.8L_{1_nom}, L_2 = 1.2L_{2_nom}, where L_{1_nom} and L_{2_nom} are the nominal values of L_1 and L_2, respectively.

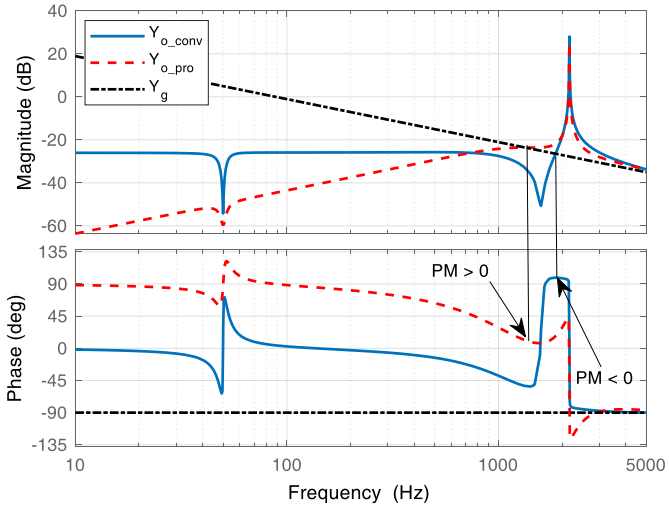

Fig. 8. The Bode plots of the output admittances for the conventional method (Y_{o_conv}), proposed method (Y_{o_pro}), and grid admittance (Y_g).

Fig. 7 shows the closed-loop poles of the control system with the proposed WAC control method for Case A and Case B under the grid impedance variations, while K_w is selected based on the nominal values of L_1 and L_2 (L_{1_nom} and L_{2_nom}). As Fig. 7(a) shows, the system keeps its stability in Case A irrespective of tolerances of L_1 and L_2, since all poles are inside the unit circle. From Fig. 7(b), it could be found that the system is unstable when the inverter is connected to a stiff grid (L_g = 0). However, the system becomes stable immediately with the increase of the grid impedance. However, such a single condition (L_g = 0) hardly challenges the system stability since inverters rarely connect to a very stiff grid with zero grid impedance. Overall, it could be concluded that the system has a good performance against the parameters tolerances.

D. Impedance-Based Stability

For the sake of generality, the inverter output admittance $Y_o(s)$ is derived using Fig. 5 as (19), to examine the stability of the inverter in different cases.

$$Y_o(s)\Big|_{\substack{i_{ref}=0\\ z_g=0}} = \frac{Z_{L1}+Z_C+K_wG_i(s)G_d(s)K_{PWM}-G_{ff}(s)G_d(s)K_{PWM}Z_C}{Z_{L1}Z_{L2}+Z_{L1}Z_C+Z_{L2}Z_C+G_i(s)G_d(s)K_{PWM}(K_wZ_{L2}+Z_C)} \tag{19}$$

Fig. 8 shows the Bode plot of $Y_o(s)$ using the proposed WAC control method, as well as inverter output admittance using the conventional WAC control method (supposing G_{ff} = 0 in (19)) and also, the Bode plot of grid admittance (Y_g) for L_g = 1.8 mH. Regarding impedance-based stability criterion [37], two stable subsystems can work stably in parallel if they have a positive phase margin (PM) at the intersection point of their output admittances in the Bode plot.

$$\mathrm{PM} = 180° - [\angle Y_o(f_i) - \angle Y_g(f_i)]. \tag{20}$$

This article has been accepted for publication in a future issue of this journal, but has not been fully edited. Content may change prior to final publication. Citation information: DOI 10.1109/JESTIE.2021.3108511, IEEE Journal of Emerging and Selected Topics in Industrial Electronics

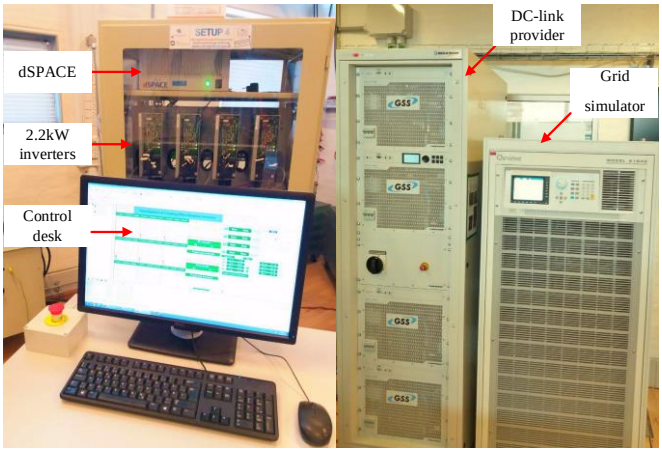

Fig. 9. Experimental setup.

As shown in Fig. 8, by using the suggested method, the phase of Y_{o_pro} is lower than 90° at high frequencies. Thus, grid impedance variations never make the system unstable since the PM is always positive according to (20) and the inverter will have a stable operation regardless of the grid impedance value. It shows the suggested approach can improve the system stability in the cases that grid impedance changes widely. However, it can be also observed in Fig. 8 that by employing the conventional WAC control method, the phase of the output admittance exceeds 90° at the vicinity of the resonance frequency. It will impair the system stability if the inverter and grid intersect in this region, as it happens in Fig. 8 for L_g = 1.8 mH, for instance. It shows that the conventional WAC method may lose its stability when the grid impedance varies.

IV. Experimental Results

To evaluate the analysis and performance of the suggested WAC control method and show the drawbacks of the conventional one, the experimental tests are carried out using a laboratory setup as shown in Fig. 9. The control algorithm is implemented using the *dSPACE* DS1006. Also, a *Danfoss* inverter with 2.2kW rated power is used, and grid-simulator *Chroma 61845* acts as an ideal utility grid. The harmonic content of waveforms is analyzed by *FLUKE 437*. The system and control parameters are the same as those presented in Tables I and II, respectively.

To validate the performance of the proposed method an experiment is carried out under a grid impedance variation. In this experiment, L_g changes suddenly from 0 to 1.8 mH. Fig. 10 shows the grid injected current in this situation. As it could be seen, the system remains stable despite grid impedance variations, which implies that the system has good robustness and performance in weak grids.

The above-mentioned scenario is tested again but by using the conventional WAC control method and Fig. 11 shows its related result. It could be observed that the system loses its stability after the grid impedance variation. The experimental results validate the analysis regarding Figs. 6 and 8. Also, another test is carried out to validate the analytical results of

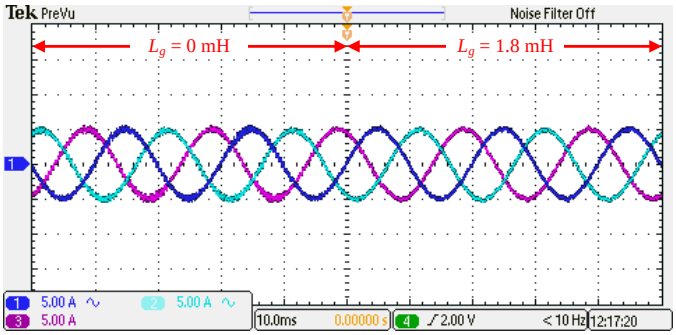

Fig. 10. The grid injected current using the improved WAC control method.

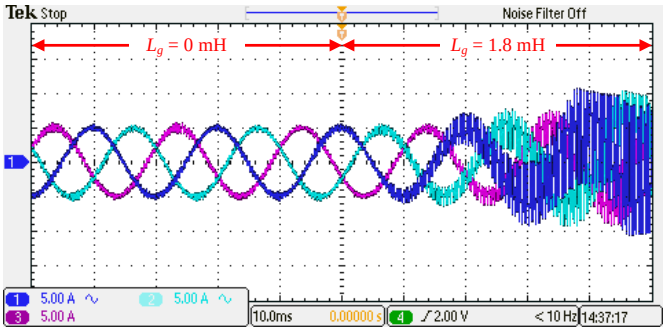

Fig. 11. The grid injected current using the conventional WAC control method while the grid inductance varies from 0 to 1.8mH.

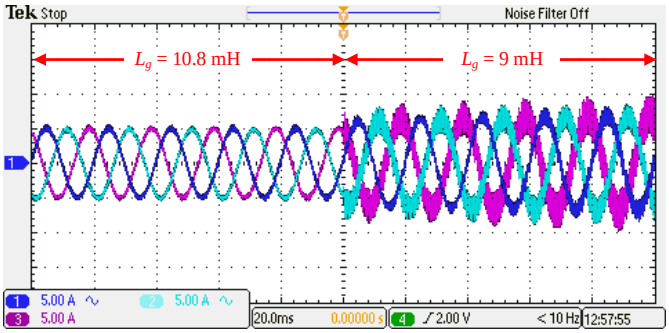

Fig. 12. The grid injected current using the conventional WAC control method while the grid inductance varies from 10.8mH to 9mH.

Fig. 3. In this test, the grid inductance is changed from 10.8 mH to 9 mH. Fig. 12 shows the experimental results. As could be observed, the system works stably when L_g = 10.8 mH, however, it becomes unstable by reducing L_g.

To evaluate the transient behavior of the improved WAC control method, a step change is applied to the reference current from half to full load for both cases i.e., L_g = 0 and L_g = 1.8 mH, and its related results are presented in Fig. 13. It could be found that in the case of L_g = 0, it takes a longer time for transient oscillations to decay because of critical stability at this point.

The current harmonic spectrum for both cases i.e., L_g = 0 and L_g = 1.8 mH in the steady-state condition are given in Fig. 14 (a) and (b), respectively. It shows that the grid injected current in the case of L_g = 0, has higher harmonic contents in comparison with L_g = 1.8 mH. However, such a single point could be ignored since inverters rarely connect to a very stiff grid with zero grid impedance.

This article has been accepted for publication in a future issue of this journal, but has not been fully edited. Content may change prior to final publication. Citation information: DOI 10.1109/JESTIE.2021.3108511, IEEE Journal of Emerging and Selected Topics in Industrial Electronics

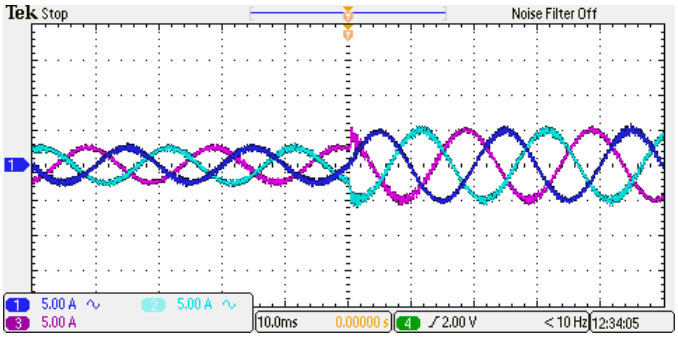

(a)

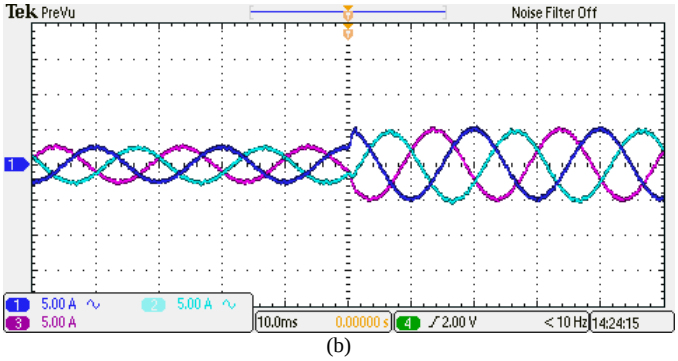

(b)

Fig. 13. Transient behavior of the grid injected current. (a). L_g = 0. (b) L_g = 1.8 mH.

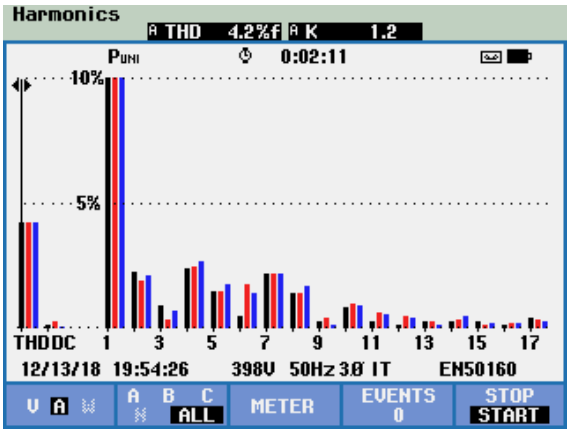

(a)

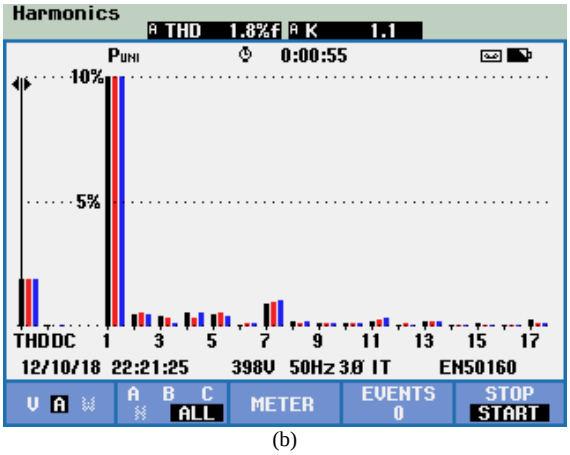

(b)

Fig. 14. The harmonic spectrum of the current. (a). L_g = 0. (b) L_g = 1.8 mH.

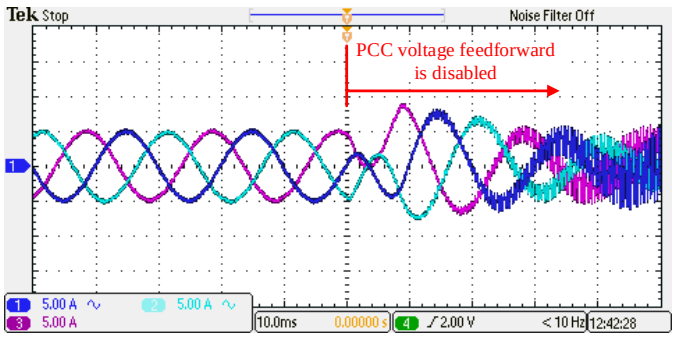

Fig. 15. The grid injected current with and without the feedforward method.

Another experiment is carried out to evaluate the effectiveness of the PCC voltage feedforward loop. In this test, the control system employs the PCC voltage feedforward loop at first, and then, it is disabled. It should be noted that L_g = 1.8 mH is considered for this experiment. The related results are presented in Fig. 15. As expected, the system becomes unstable when the PCC voltage feedforward loop is disabled. In fact, by disabling the PCC voltage feedforward loop, the control system turns into a conventional WAC control system, which is very sensitive to the grid impedance. This experiment shows how the introduced PCC voltage feedforward method affects the system stability. The proposed method is simple and does not burden the computational task. Also, it does not need any extra sensors, because the PCC voltage is normally used for the synchronization of the inverter and the grid. However, it improves the stability and robustness of the WAC control method whereas it inherits the merits of the conventional method.

VI. Conclusion

An improved WAC control method based on using the PCC voltage feedforward is presented in this paper. Unlike inverter- or grid-side current control methods that suffer from the delay and also, the critical frequency that impairs the stability in those methods, the proposed control system does not depend on the delay. It shows that although the conventional WAC control method degrades the order of the system, however, it is sensitive to the grid impedance variations. Since using grid impedance estimation methods are not reasonable because of additional computational effort, a feedforward method is introduced, which employes the PCC voltage and addresses the problems of the conventional WAC control method. The suggested WAC method does not need any knowledge about the grid impedance and has strong robustness against the grid impedance variations. It is worth mentioning that in the suggested approach there is no need for any extra sensors which in turn, save the costs in comparison with conventional methods. The performance of the proposed method is verified using comprehensive analysis and experimental results.

REFERENCES

[1] S. Jayalath and M. Hanif, "Generalized *LCL*-filter design algorithm for grid-connected voltage-source inverter," *IEEE Trans. Ind. Electron.*, vol. 64, no. 3, pp. 1905–1915, Mar. 2017.

[2] Y. Han, M. Yang, H. Li, P. Yang, L. Xu, E. A. A. Coelho, and J. M. Guerrero "Modeling and stability analysis of *LCL*-type grid-connected inverters: A comprehensive overview," *IEEE Access*, vol. 7, pp. 114975-115001, 2019.

[3] R. Peña-Alzola, M. Liserre, F. Blaabjerg, R. Sebastián, J. Dannehl, and F. W. Fuchs, "Analysis of the passive damping losses in *LCL*-filter-based grid converters," *IEEE Trans. Power Electron.*, vol. 28, no. 6, pp. 2642-2646, Jun. 2013.

[4] J. Dannehl, C. Wessels, and F. W. Fuchs, "Filter-based active damping of voltage source converters with *LCL* filter," *IEEE Trans. Ind. Electron.*, vol. 58, no. 8, pp. 3623–3633, Aug. 2011.

[5] A. Akhavan, Saeed Golestan, J. C. Vasquez, J. M. Guerrero, and C. Xie, "Stability enhancement of inverters in grid-connected microgrids using FIR filter," *IEEE J. Emerg. Sel. Topics Ind. Electron.*, vol. 2, no. 2, pp. 122-131, Apr. 2021.

[6] X. Wang, F. Blaabjerg, and P. C. Loh, "Grid-current-feedback active damping for *LCL* resonance in grid-connected voltage-source converters," *IEEE Trans. Power Electron.*, vol. 31, no. 1, pp. 213-223, Jan. 2016.

[7] D. Pan, X. Ruan, C. Bao, W. Li, and X. Wang, "Capacitor-current-feedback active damping with reduced computation delay for improving robustness of *LCL*-Type grid-connected inverter," *IEEE Trans. Power Electron.*, vol. 29, no. 7, pp. 3414–3427, Jul. 2014.

[8] S. Y. Park, C. L. Chen, J. S. Lai, and S. R. Moon, "Admittance compensation in current loop control for a grid-tie *LCL* fuel cell inverter," *IEEE Trans. Power Electron.*, vol. 23, no. 4, pp. 1716–1723, Jul. 2008.

[9] Y. Jia, J. Zhao, and X. Fu, "Direct grid current control of *LCL*-filtered grid-connected inverter mitigating grid voltage disturbance," *IEEE Trans. Power Electron.*, vol. 29, no. 3, pp. 1532–1541, Mar. 2014.

[10] Z. Zou, Z. Wang, and M. Cheng, "Modeling, analysis, and design of multifunction grid-interfaced inverters with output *LCL* filter," *IEEE Trans. Power Electron.*, vol. 29, no. 7, pp. 3830–3839, Jul. 2014.

[11] R. P. Alzola, M. Liserre, F. Blaabjerg, M. Ordonez, and T. Kerekes, "A self-commissioning notch filter for active damping in a three-phase *LCL* filter-based grid-tie converter," *IEEE Trans. Power Electron.*, vol. 29, no. 12, pp. 6754–6761, Dec. 2014.

[12] A. Akhavan, J. C. Vasquez, and J. M. Guerrero, "A simple method for passivity enhancement of current controlled grid-connected inverters," *IEEE Trans. Power Electron.*, vol. 35, no. 8, pp. 7735-7741, Aug. 2020.

[13] X. Ruan, X. Wang, D. Pan, D. Yang, W. I. Li, and C. Bao, "Resonance damping methods of *LCL* filter," in *Control Techniques for LCL-Type Grid-Connected Inverters*. Beijing, China: Springer, 2018, ch. 8, pp. 165–196.

[14] Z. Xin, X. Wang, P. C. Loh, and F. Blaabjerg, "Grid-current-feedback control for *LCL*-filtered grid converters with enhanced stability," *IEEE Trans*. *Power Electron.*, vol. 32, no. 4, pp. 3216-3228, Apr. 2017.

[15] A. Akhavan, H. R. Mohammadi, J. C. Vasquez, and J. M. Guerrero, "Passivity-based design of plug-and-play current-controlled grid-connected inverters," *IEEE Trans. Power Electron*, vol. 35, no. 2, pp. 2135-2150, Feb. 2020.

[16] D. Pan, X. Ruan, C. Bao, W. Li, and X. Wang, "Capacitor-current-feedback active damping with reduced computation delay for improving robustness of *LCL*-type grid-connected inverter," *IEEE Trans*. *Power Electron*., vol. 29, no. 7, pp. 3414–3427, Jul. 2014.

[17] X. Li, X. W. Y. Geng, X. Yuan, C. Xia, and X. Zhang, "Wide damping region for *LCL*-type grid-connected inverter with an improved capacitor current- feedback method," *IEEE Trans. Power Electron.*, vol. 30, no. 9, pp. 5247–5259, Sep. 2015.

[18] V. Miskovic, V. Blasko, T. Jahns, A. Smith, C. Romenesko, "Observer-based active damping of *LCL* resonance in grid-connected voltage source converters" in *Proc. IEEE Energy Convers. Congr. Expo*., 2013, pp. 4850–4856.

[19] L. Zhou, Y. Chen, A. Luo, J. M. Guerrero, X. Zhuo, Z. Chen, and W. Wu, "Robust two degrees-of-freedom single-current control strategy for *LCL*-type grid-connected DG system under grid-frequency fluctuation and grid-impedance variation," *IET Power Electron.*, vol. 9, no. 14, pp. 2682–2691, Nov. 2016.

[20] J. Rodriguez *et al.*, "State of the art of finite control set model predictive control in power electronics," *IEEE Trans. Ind. Informat.*, vol. 9, no. 2, pp. 1003–1016, May 2013.

[21] N. Kumar, T. K. Saha, and J. Dey, "Sliding-mode control of PWM dual inverter-based grid-connected PV system: Modeling and performance analysis," *IEEE J. Emerg. Sel. Topics Power Electron.*, vol. 4, no. 2, pp. 435-444, Jun. 2016.

[22] G. Shen, D. Xu, L. Cao, and X. Zhu, "An Improved control strategy for grid-connected voltage source inverters with an *LCL* filter," *IEEE Trans. Power Electron.*, vol. 23, no. 4, pp. 1899–1906, Jul. 2008.

[23] G. Shen, X. Zhu, J. Zhang, and D. Xu, "A new feedback method for PR current control of *LCL*-filter-based grid-connected inverter," *IEEE Trans. Ind. Electron.*, vol. 57, no. 6, pp. 2033−2041, Jun. 2010.

[24] J. He, Y. W. Li, D. Xu, X. Liang, B. Liang, and C. Wang, "Deadbeat weighted average current control with corrective feed-forward compensation for microgrid converters with nonstandard *LCL* filter," *IEEE Trans. Electron.*, vol. 32, no. 4, pp. 2661−2674, Apr. 2017.

[25] N. He, D. Xu, Y. Zhu, J. Zhang, G. Shen, Y. Zhang, J. Ma, and C. Liu, "Weighted average current control in a three-phase grid inverter with an *LCL* filter," *IEEE Trans. Power Electron.*, vol. 28, no. 6, pp. 2785−2797, Jun. 2013.

[26] M. S. Munir, J. He, and Y. W. Li, "Comparative analysis of closed-loop current control of grid connected converter with *LCL* filter," in *Proc. IEEE Int. Electr. Mach. Drives Conf.*, 2011, pp. 1641–1646.

[27] D. K. Alves, R. L. A. Ribeiro, F. B. Costa, and T. O. A. Rocha, "Real-time wavelet-based grid impedance estimation method," *IEEE Trans. Ind. Electron.*, vol. 66, no. 10, pp. 8263–8265, Oct. 2019.

[28] P. García, M. Sumner, Á. Navarro-Rodríguez, J. M. Guerrero, and J. García, "Observer-based pulsed signal injection for grid impedance estimation in three-phase systems", *IEEE Trans. Ind. Electron.*, vol. 65, no. 10, pp. 7888-7899, Oct. 2018.

[29] D. Pan, X. Ruan, X. Wang, H. Yu, and Z. Xing, "Analysis and design of current control schemes for *LCL*-type grid-connected inverter based on a general mathematical model," *IEEE Trans. Power Electron.*, vol. 32, no. 6, pp. 4395–4410, Jun. 2017.

[30] J. Xu and S. Xie, "Optimization of weighted current control for grid-connected *LCL*-filtered inverters," in *Proc. IEEE ECCE Asia Downunder*, 2013, pp. 1170–1175.

[31] Y. Han, Z. Li, P. Yang, C. Wang, L. Xu, and J. M. Guerrero, "Analysis and design of improved weighted average current control strategy for *LCL*-type grid-connected inverters," *IEEE Trans. Energy Convers.*, vol. 32, no. 3, pp. 941−952, Sep. 2017.

[32] D. Pan, X. Ruan, X. Wang, F. Blaabjerg, X. Wang, Q. Zhou, "A highly robust single-loop current control scheme for grid-connected inverter with an improved *LCCL* filter configuration", *IEEE Trans. Power Electron.*, vol. 33, no. 10, pp. 8474−8487, Oct. 2018.

[33] C. Bao, X. Ruan, X. Wang, W. Li, D. Pan, and K. Weng, "Step-by-step controller design for *LCL*-type grid-connected inverter with capacitor-current feedback active-damping," *IEEE Trans. Power Electron.*, vol. 29, no. 3, pp. 1239–1253, Mar. 2014.

[34] A. G. Yepes, A. Vidal, J. Malvar, O. López, and J. D.-Gandoy, "Tuning method aimed at optimized settling time and overshoot for synchronous proportional-integral current control in electric machines," *IEEE Trans. Power Electron.*, vol. 29, no. 6, pp. 3041–3054, Jun. 2014.

[35] D. G. Holmes, T. A. Lipo, B. P. McGrath, and W. Y. Kong, "Optimized design of stationary frame three phase AC current regulators," *IEEE Trans. Power Electron.*, vol. 24, no. 11, pp. 2417–2426, Nov. 2009.

[36] A. G. Yepes, F. D. Freijedo, J. Doval-Gandoy, O. Lopez, J. Malvar, Fernandez-Comesana, "Effects of discretization methods on the performance of resonant controllers", *IEEE Trans. Power Electron.*, vol. 25, no. 7, pp. 1692-1712, Jul. 2010.

[37] J. Sun, "Impedance-based stability criterion for grid-connected inverters," *IEEE Trans. Power Electron.*, vol. 26, no. 11, pp. 3075-3078, Nov. 2011.

Ali Akhavan (Member, IEEE) received the B.S., M.S., and Ph.D. degrees in electrical engineering from University of Kashan, Kashan, Iran in 2012, 2014, and 2019, respectively. Since August 2019, he has been with Aalborg University, Aalborg, Denmark, where he is currently a Postdoctoral Fellow with the Department of Energy Technology. His research interests include power electronics, modeling and control of grid-connected converters, stability analysis, and microgrid clusters.

Juan C. Vasquez (Senior Member, IEEE) received the B.S. degree in electronics engineering from the Autonomous University of Manizales, Manizales, Colombia, in 2004, and the Ph.D. degree in automatic control, robotics, and computer vision from BarcelonaTech-UPC, Spain, in 2009. He was Assistant Professor and Associate Professor with the Department of Energy Technology, Aalborg University, Denmark, in 2011 and 2014, respectively. In 2019, he became Professor in energy internet and microgrids. Currently, he is the Co-Director of the Villum Center for Research on Microgrids (CROM). He was a Visiting Scholar with the Center of Power Electronics Systems (CPES), Virginia Tech, U.S.A. and a Visiting Professor with Ritsumeikan University, Japan. He has published more than 450 journal papers in the field of microgrids, which in total are cited more than 19000 times. His current research interests include operation, advanced hierarchical and cooperative control, optimization and energy management applied to distributed generation in ac/dc microgrids, maritime microgrids, advanced metering infrastructures, and the integration of Internet of Things and energy Internet into the SmartGrid.

Josep M. Guerrero (Fellow, IEEE) received the B.S. degree in telecommunications engineering, the M.S. degree in electronics engineering, and the Ph.D. degree in power electronics from the Technical University of Catalonia, Barcelona, Spain, in 1997, 2000, and 2003, respectively. Since 2011, he has been a Full Professor with the Department of Energy Technology, Aalborg University, Aalborg, Denmark, where he is responsible for the Microgrid Research Program. From 2014, he has been a Chair Professor with Shandong University; from 2015, he has been a Distinguished Guest Professor with Hunan University; and from 2016, he has been a Visiting Professor Fellow with Aston University, Birmingham, U.K.; and a Guest Professor with the Nanjing University of Posts and Telecommunications, Nanjing, China. From 2019, he has been a Villum Investigator by The Villum Fonden, Søborg, Denmark, which supports the Center for Research on Microgrids (CROM), Aalborg University, being the founder and Director of the same center. His research interests include different microgrid aspects, including power electronics, distributed energy-storage systems, hierarchical and cooperative control, energy management systems, smart metering and the Internet of Things for ac–dc microgrid clusters and islanded minigrids. He has authored or coauthored more than 600 journal papers in the fields of microgrids and renewable energy systems, which are cited more than 50000 times. His research specially focuses on microgrid technologies applied to offshore wind, maritime microgrids for electrical ships, vessels, ferries and seaports, and space microgrids applied to nanosatellites and spacecrafts.